藤崎誠一郎、藤崎彩恵子、伊部史朗、浅黄司、伊藤俊広、吉田繁、小池隆夫、大家正泰、渡邊香奈子、正兼亜季、上田幹夫、潟永博之、松田昌和、貞升健志、長島真美、岡田清美、近藤真規子、秦 眞美、溝上泰司、森 治代、南 留美、白阪琢磨、岡慎一、杉浦 亙、金田次弘	日本における HIV-1 遺伝子型薬剤耐性検査のコントロールサーベイ	日本エイズ学会誌	9	136-146	2007
Takahashi M, Ibe S, Kudaka Y, Okumura N, Hirano A, Suzuki T, Mamiya N, Hamaguchi M, Kaneda T.	No observable correlation between central nervous system side effects and EFV plasma concentration in Japanese HIV-1 infected patients treated with EFV containing HAART.	AIDS Res. Hum. Retroviruses	23	983-987	2007
平野 淳、奥村直哉、久高祐一、寺畑奈美、高橋昌明、坂野和英、横幕能行、安岡彰、間宮均人、濱口元洋、金田次弘	サイトメガロウイルス感染症を発症した日本人エイズ患者に対するバルガンシクロビルの効果および安全性についての評価	日本病院薬剤師会雑誌	43	1397-1399	2007

Takahashi M, Kudaka Y, Okumura N, Hirano A, Banno K, Kaneda T.	Determination of plasma tenofovir concentrations using a conventional LC-MS method.	Biol. Pharm. Bull.	30	1784-1786	2007
Takahashi M, Kudaka Y, Okumura N, Hirano A, Banno K, Kaneda T.	The validation of plasma darunavir concentrations determined by the HPLC method for protease inhibitors.	Biol. Pharm. Bull.	30	1947-1949	2007
小柏 均、永井裕美、近藤恭子、加堂真由、伊部史朗、一三武二郎、玉村和規、間宮均人、金田次弘	リアルタイムPCR法による *Pneumocystis jirovecii* 迅速定量法の確立	医学検査	56	1527-1534	2007
濱口元洋	免疫再構築症候群とその対応	日本エイズ学会誌	9	91-101	2007
Gatanaga H, Hayashida T, Tsuchiya K, Yoshino M, Kuwahara T, Tsukada H, Fujimoto K, Sato I, Ueda M, Horiba M, Hamaguchi M, Yamamoto M, Takata N, Kimura A, Koike T, Gejyo F, Matsushita S, Shirasaka T, Kimura S, Oka S	Successful efavirenz dose reduction in HIV type 1-infected individuals with cytochrome P450 2B6 *6 and *26	Clin. Infect. Dis.	45	1230-1237	2007

Gatanaga H, Ibe S, Matsuda M, Yoshida S, Asagi T, Kondo M, Sadamasu K, Tsukada H, Masakane A, Mori H, Takata N, Minami R, Tateyama M, Koike T, Itoh T, Imai M, Nagashima M, Gejyo F, Ueda M, Hamaguchi M, Kojima Y, Shirasaka T, Kimura A, Yamamoto M, Fujita J, Oka S, Sugiura W.	Drug-resistant HIV-1 prevalence in patients newly diagnosed with HIV/AIDS in Japan.	Antiviral Res.	75	75-82	2007
Ibe S, Fujisaki S, Fujisaki S, Morishita T, Kaneda T.	Quantitative SNP-Detection Method for Estimating HIV-1 Replicative Fitness: Application to Protease Inhibitor-Resistant Viruses.	Microbiol. Immunol.	50	765-772	2006
金田次弘	第2回HIV国際会議に参加(政策医療振興財団の助成による国際会議出席報告).	医療の広場	46	18-20	2006
間宮均人、濱口元洋	プライマリ・ケア医が対処できる合併症と専門医に送るべき合併症	治療	88	2955-2960	2006

高橋昌明、奥村直也、伊部史朗、久高祐一、溝口和代、鈴木達男、金田次弘	名古屋医療センターにおける抗 HIV 療法の変遷と TDM の有効例	日本病院薬剤師会雑誌	42	919-923	2006
濱口元洋	エイズ・HIV 感染症患者の診療と今後の課題	明日の臨床	18	1-7	2006
濱口元洋	HIV 感染症治療の現況	現代医学	54	115-122	2006
Gatanaga H, Das D, Suzuki Y. Yeh DD, Hussain KA, Ghosh AK, Mitsuya H.	Altered HIV-1 Gag protein interactions with cyclophilin A(CypA) on the accuisition of H219Q and H219P substitutions in the CypA binding loop.	J. Biol. Chem.	281	1241-1250	2006
白阪琢磨	増え続ける HIV 感染症とその対策	公衆衛生	70	101-105	2006
川崎美由紀、橋本修二、古金秀樹、下司有加、織田幸子、白阪琢磨	近畿ブロック拠点病院における HIV/AIDS 受療者の居住地、紹介元と転院先	日本エイズ学会誌	8	34-40	2006
Minami R, Takahama S, Yamamoto M.	RCAS1 induced by HIV-Tat is involved in the apoptosis of HIV-1 infected and uninfected CD4+ T cells.	Cellular Immunology	243	41-47	2006
南　留美 山本政弘	Elevated serum levels of RCAS 1 are associated with Poor recovery of CD4+T cell count after ART in HIV-1-infected patients.	日本エイズ学会誌	8	25-27	2006
南　留美 高濱宗一郎 山本政弘	高熱、リンパ節腫脹を繰り返したのち発症した HIV-1 陽性 HHV-8 関連 Castleman 病の 1 例	感染症学雑誌	80	423-427	2006

III. 研究成果の刊行物・別刷

9

PNA–*In Situ* Hybridization Method for Detection of HIV-1 DNA in Virus-Infected Cells and Subsequent Detection of Cellular and Viral Proteins

Tomoko Hagiwara, Junko Hattori, and Tsuguhiro Kaneda

Summary

We describe *in situ* hybridization protocols using peptide nucleic acid (PNA) as a probe for detecting HIV-1 DNA in virus-infected cells and the subsequent detection of cellular and/or viral proteins. Because a PNA probe of approx 20 bases was sufficiently long to detect a specific target sequence, a conserved sequence of such a short length was easily identified. Therefore, this probe is valuable even to identify quasi-species of HIV-1. In addition, we adopted a catalyzed signal amplification method to amplify weak viral DNA signals; thus, stringent washing was crucial for eliminating false-positive signals. Our double-staining method using PNA–*in situ* hybridization and subsequent immunostaining enabled the active and inactive proviruses to be distinguished.

Key Words: *In situ* hybridization; peptide nucleic acid; catalyzed signal amplification; HIV-1 provirus; CD4-positive T lymphocytes; p24; HLA-DR.

1. Introduction

In situ hybridization (ISH) is now popularly used in cytogenetic studies to determine the localization of a specific gene on a chromosome and to detect mRNA expression and viral infection within cells using DNA or RNA probes. Nonradioactive ISH methods using fluorescence or visible light to visualize signals generally are used for the detection of target nucleic acid sequences. In general, probes of more than 500 bp in length are required in such studies *(1)*.

Until recently, the detection of HIV-1 has been performed by using autoradiography, using probes labeled with radioisotopes, such as ^{35}S *(2–4)* and ^{125}I *(2,5)*. Although the use of radioactive ISH for the detection of HIV-1 is time consuming and not very convenient, the small copy number of HIV-1 in

From: *Methods in Molecular Biology, vol. 326:* In Situ *Hybridization Protocols: Third Edition*
Edited by: I. A. Darby and T. D. Hewitson © Humana Press Inc., Totowa, NJ

infected cells has hindered the development of a conventional nonradioactive detection system. In addition, designing a suitable proper probe with a length of more than 150 bp is very difficult because of the general lack of long-conserved DNA sequences in viruses, such as HIV-1, that have error-prone reverse transcriptase without any repair activity. To bypass this problem, we developed a peptide nucleic acid (PNA) that mimics the DNA configuration *(6–8)*. PNA, being electrically neutral, can penetrate into cells more easily than DNA and, in addition, PNA can more strongly hybridize with DNA than DNA *(9,10)*. For these reasons, a PNA probe of approx 20 bases in length is long enough to detect a specific target sequence *(11)*.

To overcome the weak viral DNA signal, one of the following methods for signal amplification can be used: one is *in situ* polymerase chain reaction (PCR *[12]*), and the other is a catalyzed signal amplification (CSA) using biotinyl tyramide *(13)*. *In situ* PCR is quite powerful for amplification of rare target DNA within cells; therefore, *in situ* PCR-driven ISH would be suitable for detecting low copy number DNA sequences. However, this method carries the risk of amplicons synthesized *in situ* diffusing and resulting in false-positives *(14)*. On the other hand, a single copy of the HPV-16 virus was detected successfully using the CSA method *(14)*. Therefore, we adopted the CSA method for detecting HIV-1 DNA *(15)* and incorporated a crucial stringent washing step to eliminate nonspecific signals that arise from the CSA procedure.

Here, we describe the procedures for detecting HIV-1 DNA in infected CD4-positive T lymphocytes, and the phenotypic determination of HIV-1 DNA-positive cells by a double staining method.

2. Materials

2.1. Cell Lines

1. ACH2: positive control. Human lymphoid cell line latently infected with HIV-1.
2. MOLT4-IIIB: positive control. Human leukemic cell line persistently infected with HIV-1 strain IIIB.
3. MOLT4: negative control.

2.2. Sample Preparation

2.2.1. CD4-Positive T-Lymphocytes Smears

1. StemSep column chromatography (Stem Cell Technologies, Inc., Vancouver, BC, Canada; cat. no. STS-14032).
2. Phosphate-buffered saline (PBS) with 3% fetal bovine serum.
3. 4% paraformaldehyde (PFA) containing 0.1 *M* sodium phosphate buffer, pH 7.4.
4. Ethanol.
5. Silane-coated slides.

6. Wax pen (DakoCytomation A/S, Glostrup, Denmark).
7. Staining racks and containers.
8. Dryer.

2.2.2. Formalin-Fixed, Paraffin-Embedded Tissue Sections

1. Tissue blocks of 20% formalin-fixed or 4% PFA-fixed, paraffin-embedded samples.
2. Silane-coated slides.
3. Staining racks and containers.
4. Xylene.
5. Rehydration series: 100, 95, 90, and 70% ethanol.

2.3. Pretreatment

2.3.1. CD4-Positive T Lymphocytes Smears

1. Tris-buffered saline containing Tween-20 (TBST): 50 m*M* Tris-HCl, 300 m*M* NaCl, 0.1% Tween-20, pH 7.6.
2. Target retrieval solution (DakoCytomation A/S; cat. no. S1700).
3. Methanol containing 0.3% H_2O_2.
4. Water bath.
5. Staining racks and plastic containers.

2.3.2. Formalin-Fixed, Paraffin-Embedded Tissue Sections

1. The same as **Subheading 2.3.1., items 1–5.**
2. Proteinase K (DakoCytomation A/S, S3004).

2.4. Preparation of PNA Probe

1. PNA probe: the structure of the probe is as follows: FITC·HN-GCAGCTTCCT-CATTGATGG-$CONH_2$ (FASMAC Co. Ltd., Kanagawa, Japan; *see* **Note 1**).
2. DNA ISH solution (DakoCytomation A/S; cat. no. S3305).
3. Cover slips.

2.5. Heat Denaturation

1. Hotplate.

2.6. Hybridization

1. Stringent wash solution (DakoCytomation A/S; cat. no. K5201).
2. TBST.
3. Incubator.
4. Plastic containers.
5. Water bath.
6. Moist chamber.

2.7. PNA Probe Detection by CSA

1. Horseradish peroxidase (HRP)-conjugated anti-FITC antibody (DakoCytomation A/S; cat. no. P5100).
2. Biotinyl tyramide solution (DakoCytomation A/S, GenPoint kit K0620).
3. HRP-conjugated streptavidin (DakoCytomation A/S, GenPoint kit K0620).
4. Alexa Fluor 488-labeled streptavidin (Invitogen, Carlsbad, CA).
5. 4,6-diamino-2-phenylindole (DAPI) II (Vysis, Inc., Downers Grove, IL).
6. TBST.
7. Staining racks and containers.
8. Cover slips.

2.8. PNA–ISH and Immunohistochemistry (IHC) (Indirect Method)

1. Mouse anti-human CD4 monoclonal antibody (Novocastra Laboratories, Ltd., Newcastle, UK; cat. no. NCL-CD4-1F6) or mouse anti-human HLA-DR monoclonal antibody (DakoCytomation A/S; cat. no. M0746).
2. Alexa Fluor 594-labeled goat anti-mouse IgG antibody (Invitrogen; cat. no. A-11005).
3. DAPI II (Vysis, Inc.).
4. Cover slips.

2.9. PNA–ISH and IHC (Labeled Streptavidin-Biotin Method)

1. Avidin solution (DakoCytomation A/S; cat. no. X0590).
2. Biotin solution (DakoCytomation A/S; cat. no. X0590).
3. Mouse monoclonal anti-HIV-1 p24 antibody (DakoCytomation A/S; cat. no. M0857).
4. Biotinylated goat anti-mouse Ig antibody (DakoCytomation A/S; cat. no. E0433).
5. Alexa Fluor 594-labeled streptavidin (Molecular Probes, Inc.; cat. no. S-11227).
6. DAPI II (Vysis, Inc.).
7. Cover slips.

3. Methods

3.1. Sample Preparation (see Note 2)

3.1.1. CD4-Positive T Lymphocytes Smears

1. Negatively select and purify CD4-positive T lymphocytes by StemSep column chromatography according to the manufacturer's instructions.
2. Spin down the collected cells at 250*g* for 5 min.
3. Discard supernatant and resuspend with PBS.
4. Mark the area for sample-mount on a silane-coated slide with a wax pen. Drop 5 µL of the cell suspension onto the slide and spread it out gently using the pipet tip.
   The area of the sample-mount (15 × 15 mm).
5. Dry the slides using a dryer at a cool setting.
6. Fix the slides with 4% PFA containing 0.1 mol/L sodium phosphate buffer, pH 7.4, at room temperature for 60 min or at 4°C overnight.

7. Rinse the slides in PBS (3 min, three times).
8. Dehydrate the slides in absolute ethanol and then store at –20°C until use.

3.1.2. Formalin-Fixed, Paraffin-Embedded Tissue Sections

1. Place a 4- to 5-µm section onto a slide. Heat the slide to melt the paraffin in a 60°C oven for 15 min and dry at 37°C overnight.
2. Deparaffinize sections in fresh xylene (3 min, three times) and rehydrate in graded (100, 100, 95, 90, and 70%) ethanols and autoclaved water.

3.2. Pretreatment

3.2.1. CD4-Positive T-Lymphocyte Smears

1. Immerse the slides in autoclaved water for 5 min.
2. Immerse the slides in preheated target retrieval solution for 40 min at 95°C, and allow to cool for 20 min.
3. Wash the slides in autoclaved water (1 min, three times).
4. Immerse the slides in methanol containing 0.3% H_2O_2 for 20 min.
5. Wash the slides in autoclaved water for 1 min.
6. Briefly immerse slides in 95% ethanol and allow to air dry.

3.2.2. Formalin-Fixed, Paraffin-Embedded Tissue Sections

1. Immerse the slides in autoclaved water for 5 min.
2. Immerse the slides in preheated target retrieval solution for 40 min at 95°C and allow to cool for 20 min.
3. Wash the slides in autoclaved water (1 min, three times).
4. Digest sections with proteinase K for 10 min at room temperature (*see* **Note 3**).
5. Wash the slides in autoclaved water (1 min, three times).
6. Treat the slides with methanol containing 0.3% H_2O_2 for 20 min.
7. Wash the slides in autoclaved water for 1 min.
8. Briefly immerse the slides in 95% ethanol and allow to air-dry.
9. Mark the area of the section with a wax pen.

3.3. Preparation of PNA Probe

1. Dilute FITC-conjugated PNA probe in hybridization solution to a final concentration of between 0.2 and 0.5 µg/mL.
2. Apply 25 µL of hybridization solution containing PNA probe to the marked area of the slide.
3. Carefully apply the cover slip, avoiding the introduction of air bubbles.

3.4. Heat Denaturation

1. Heat the slides at 93°C for 5 min on a hotplate to denature the double-stranded DNA.

3.5. Hybridization

1. Incubate the slides with the PNA probe at 45°C for 60–90 min in a moist chamber.
2. After hybridization, immerse the slides in TBST and gently remove the cover slips.

3. Wash the slides in prewarmed stringent wash solution at 57°C (20 min, twice).
4. Immerse the slides in TBST at room temperature for 5 min.

3.6. PNA Probe Detection by CSA (see Notes 4 and 5; Fig. 1)

1. Incubate HRP-conjugated rabbit anti-FITC antibody (1:500 dilution) for 60 min (*see* Note 6).
2. Wash the slides in TBST (3 min, three times).
3. Incubate biotinyl-tyramide for 15 min.
4. Wash the slides in TBST (3 min, three times).
5. Incubate HRP-conjugated streptavidin (1:600–800 dilution) for 15 min.
6. Wash the slides in TBST (3 min, three times).
7. Incubate biotinyl-tyramide for 15 min.
8. Wash the slides in TBST (3 min, three times).
9. Incubate 0.5 µg/mL Alexa Fluor 488-labeled streptavidin for 15 min in the absence of light.
10. Wash the slides in TBST in the absence of light (3 min, three times).
11. Immerse the slides in distilled water.
12. Apply DAPI II and mount cover slip.

3.7. Fluorescence Microscopy

The slides were examined under a fluorescence microscope (BX50 and BX-FLA, Olympus Corp., Tokyo, Japan) equipped with appropriate filter sets (61002, Chroma Technology Corp., Rockingham, VT). Photographic images of the fluorescent signals were taken with a CCD camera (SenSys 0400, Photometrics Ltd., Tucson, AZ) and were uploaded to a microcomputer using IPLab software (Scanalytics, Inc., Fairfax, VA). The stored images were merged to reveal various aspects (*see* **Note 7**; **Fig. 2**).

3.8. Subsequent Determination of Phenotypes After PNA–ISH Treatment

We describe here a double staining method by PNA–ISH and IHC methods for the detection of both HIV-1 DNA and a protein in the same cell, respectively. Proteins can be detected with one of two methods with IHC: an indirect method and a labeled streptavidin-biotin (LSAB) method. For the detection of CD4 or HLA-DR molecules, the conventional indirect method was used. On the other hand, the LSAB method that has higher sensitivity than the indirect method was performed to detect the p24 HIV-1 capsid protein.

Fig. 1. (*opposite page*) Schematic representation of the procedures for using the PNA-probe in the ISH method. The hybridized probe was detected by sequential reactions of the following antibodies and reagents: HRP-conjugated anti-FITC antibody, biotinylated tyramide (first amplification), HRP-labeled streptavidin, biotinylated tyramide (second amplification), and streptavidin-conjugated Alexa 488.

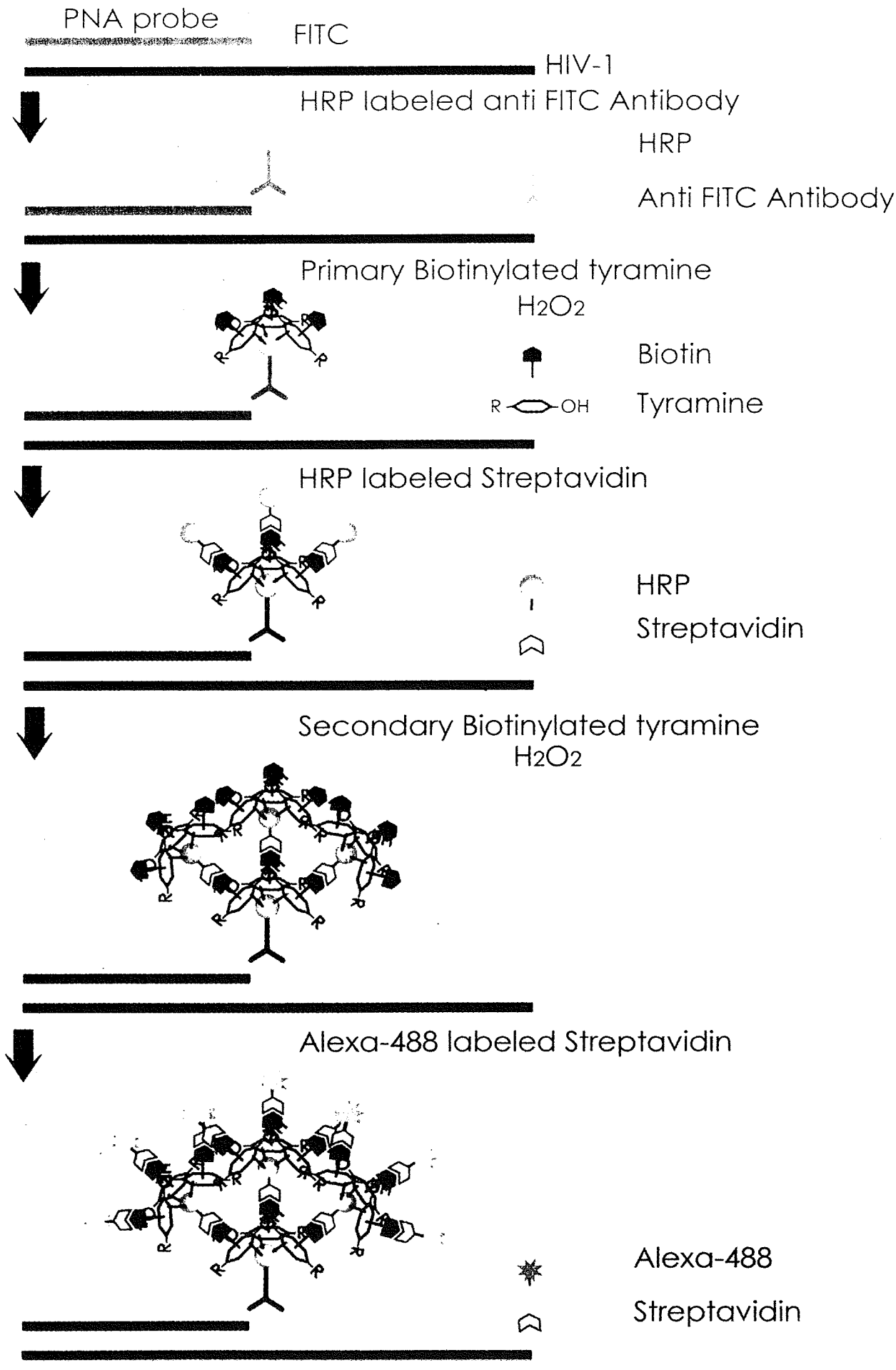
PNA probe
FITC
HIV-1
HRP labeled anti FITC Antibody
HRP
Anti FITC Antibody
Primary Biotinylated tyramine
H2O2
Biotin
Tyramine
HRP labeled Streptavidin
HRP
Streptavidin
Secondary Biotinylated tyramine
H2O2
Alexa-488 labeled Streptavidin
Alexa-488
Streptavidin

Fig. 1

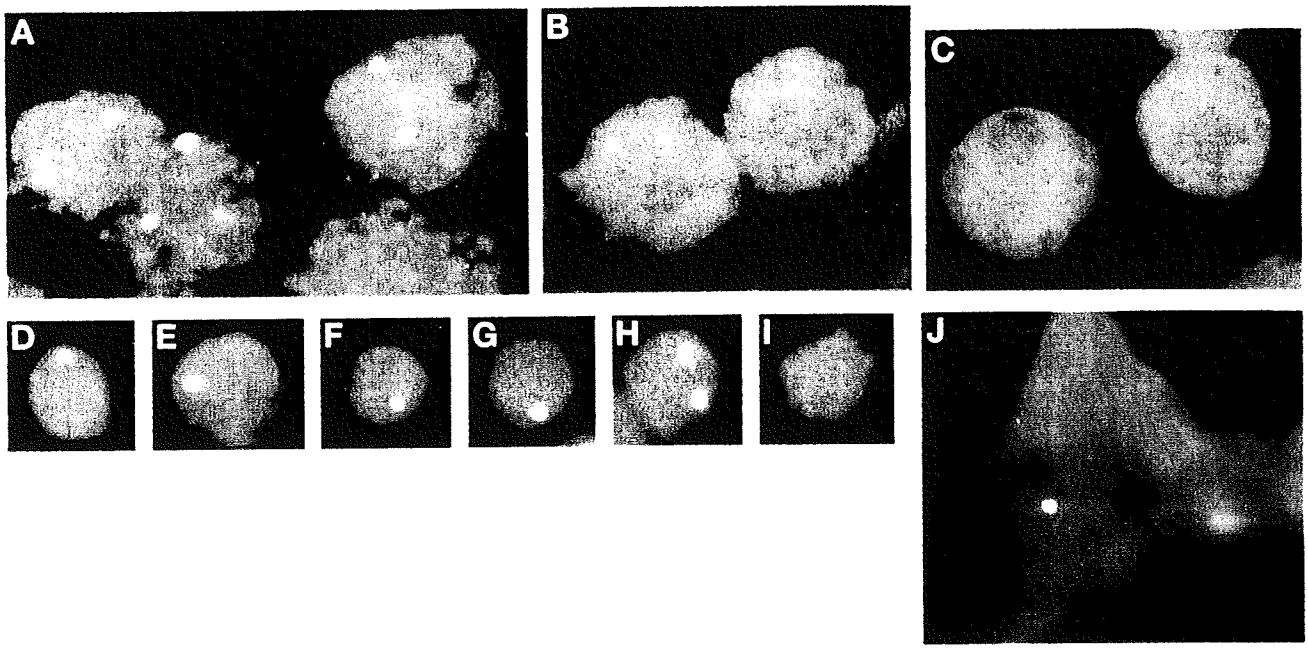

Fig. 2. Detection of HIV-1 provirus by PNA–ISH. Signals detecting HIV-1 proviruses were observed as green dots in a nucleus stained blue by DAPI. (**A**) MOLT4-IIIB. One to four proviruses per cell. (**B**) ACH2. One provirus per cell. (**C**) Negative control (MOLT4). No provirus. (**D–H**) CD4-positive T lymphocytes from HIV-1-infected patients. Most provirus-positive cells contained one provirus. Positive cells rarely contained more than two proviruses. (**I**) Negative control (CD4-positive T lymphocytes from a HIV-1-negative volunteer). No provirus. (**J**) Paraffin-embedded section of bone marrow from an AIDS patient. Positive cells contained one provirus in a nucleus.

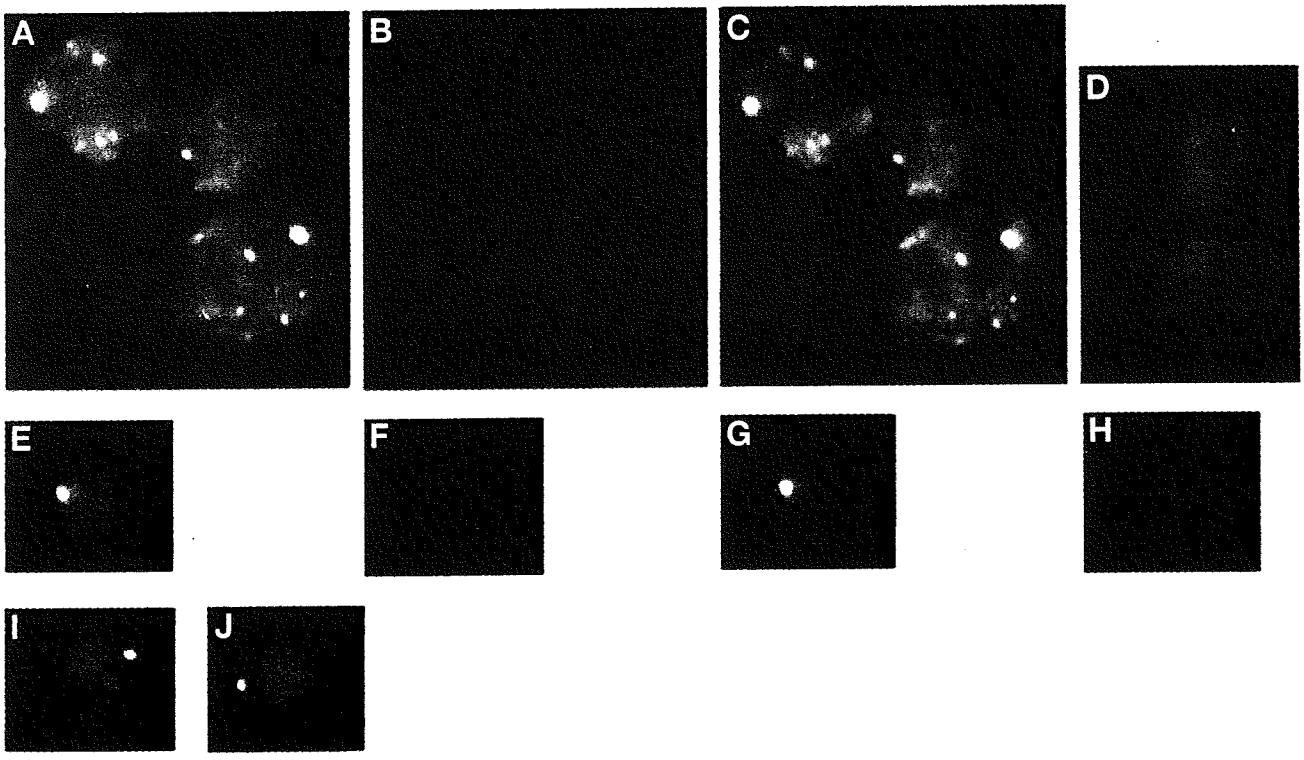

Fig. 3. Subsequent determination of phenotypes after PNA–ISH treatment. Proteins were stained red and localization of the proteins can be observed. (**A–C**) p24/HIV-1 provirus of MOLT4-IIIB. (**D**) Negative control (MOLT4). (**E–G**) p24/provirus

3.8.1. PNA–ISH and IHC (Indirect Method)

1. Follow steps 1–10 inclusive for PNA Probe Detection by CSA (Subheading 3.6.).
2. Incubate with mouse anti-human CD4 monoclonal antibody or mouse anti-human HLA-DR monoclonal antibody at 4°C overnight.
3. Wash in TBST (3 min, three times).
4. Incubate with Alexa Fluor 594-labeled goat anti-mouse IgG antibody for 30 min.
5. Wash in TBST (3 min, three times).
6. Apply DAPI II and mount a cover slip.

3.8.2. PNA–ISH and IHC (LSAB Method)

Biotin blocking of biotinyl-tyramide after PNA–ISH staining is recommended before the reaction with primary antibody for the target protein.

1. Follow **steps 1–10** inclusive for PNA Probe Detection by CSA (**Subheading 3.6.**).
2. Incubate with avidin for 10 min.
3. Wash in TBST (3 min, three times).
4. Incubate with biotin for 10 min.
5. Wash in TBST (3 min, three times).
6. Incubate with mouse monoclonal anti-HIV-1 p24 antibody at 4°C overnight.
7. Wash in TBST (3 min, three times).
8. Incubate with biotinylated goat anti-mouse Ig antibody for 30 min.
9. Wash in TBST (3 min, three times).
10. Incubate with Alexa Fluor 594-labeled streptavidin for 15 min.
11. Wash in TBST (3 min, three times).
12. Apply DAPI II and mount a cover slip.

3.8.3. Fluorescence Microscopy of Double-Stained Sample

The slides were examined under a fluorescence microscope with appropriate filter sets. Photographic images of the fluorescent signals were taken with a CCD camera, and were uploaded to a microcomputer using IPLab software. The stored images were merged to reveal various aspects (**Fig. 3**).

Fig. 3. *(continued from opposite page)* of CD4-positive T lymphocytes from HIV-1-infected patients. **(H)** Negative control (CD4-positive T lymphocytes from a HIV-1-negative volunteer). **(A,E)** provirus (green) and nucleus (blue) were merged. **(B,F)** p24 (red). p24 HIV-1 capsid proteins were observed in the cytoplasm of HIV-1 provirus positive cells. **(C,G)** provirus (green), p24 (red) and nucleus (blue) were merged. **(I,J)** CD4-positive T lymphocytes from a HIV-1-infected patient; HIV-1 provirus (green) was seen in the cell nucleus. In contrast, CD4 molecules (red) were seen in the outer-membrane **(I)** Membrane-bound or cytoplasmic HLA-DR molecules (red) were detected in HIV-1 provirus positive cells **(J)**.

4. Notes

1. The base sequence corresponds to the region from 1379 to 1397 of the HIV-1 gag gene. As the melting temperature of the anti-parallel probe is higher than that of the parallel, the use of anti-parallel type is recommended. PNA probe can be dissolved with DEPC-treated water to a concentration of 100 µg/mL, aliquotted, and stored at –20 C. A 0.01% trifluoroacetic acid can be replaced instead of water.
2. Wear gloves throughout the steps until the hybridization step is completed. Use the dry-sterilized glassware equipment and those made by stainless steel (200°C, 2 h). Use autoclaved water (121°C, 15 min) through the hybridization step.
3. To obtain an optimal concentration of proteinase K, treat fixed specimens with three different concentrations between 2 and 7 µg/mL of the enzyme.
4. This amplification method is based on the binding reaction of biotinylated tyramine to a phenol derivatives of a protein by peroxidase. This step sometimes gives nonspecific signals, therefore thorough pretreatment of specimens with methanol containing 0.3% H_2O_2 is essential to diminish the endogenous peroxidase activity. Also, it is important to stain two kinds of negative control to allow the identification of nonspecific signals: (1) HIV-1 DNA negative-specimen with a PNA probe and (2) HIV-1 DNA positive-specimen without a PNA probe (**Fig. 1**).
5. A single amplification method was successfully applied for HIV-1 RNA detection (***16***).
6. Considerable amounts of endogenous biotin is contained in liver, kidney, mucosa of digestive tract, and brain. Even in other organs, endogenous biotin becomes exposed through an activation step (*see* **Subheading 3.2.2., steps 2** and **4**). A biotin blocking of the endogenous biotin is recommended between the steps of stringent wash and HRP-FITC antibody reaction. Biotin blocking system (DakoCytomation A/S, X0590): (1) Incubate with avidin solution for 10 min, (2) wash in TBST three times for 3 min, (3) Incubate with biotin solution for 10 min, (4) wash in TBST three times for 3 min.
7. To measure the positivity of HIV-1 provirus in the CD4-positive T lymphocytes, we count 500 cells and calculate. The positivity of the HIV-1 provirus among 62 HIV-1-infected patients ranged between 0.3% and 7.9% (average of 2.7).

References

1. Webb, G. C. (2000) Radioactive *In situ* hybridization to animal chromosomes, in In Situ *Hybridization Protocols* (Darby, I. A., eds.), Humana Press, Totowa, NJ, pp. 29–50.
2. Smith, P. D., Fox, C. H., Masur, H., Winter, H. S., and Alling, D. W. (1994) Quantitative analysis of mononuclear cells expressing human immunodeficiency virus type 1 RNA in esophageal mucosa. *J. Exp. Med.* **180,** 1541–1546.
3. Brodie, S. J., Lewinsohn, D. A., Patterson, B. K., et al. (1999) In vivo migration and function of transferred HIV-1-specific cytotoxic T cells. *Nat. Med.* **5,** 34–41.

4. Fox, C. H., Kotler, D., Tierney, A., Wilson, C. S., and Fauci, A. S. (1989) Detection of HIV-1 RNA in the lamina propria of patients with AIDS and gastrointestinal disease. *J. Infect. Dis.* **159,** 467–471.
5. Haase, A. T., Retzel, E. F., and Staskus, K. A. (1990) Amplification and detection of lentiviral DNA inside cells. *Proc. Natl. Acad. Sci. USA* **87,** 4971–4975.
6. Wittung, P., Nielsen, P. E., Buchardt, O., Egholm, M., and Norden, B. (1994) DNA-like double helix formed by peptide nucleic acid. *Nature* **368,** 561–563.
7. Jensen, K. K., Orum, H., Nielsen, P. E., and Norden, B. (1997) Kinetics for hybridization of peptide nucleic acids (PNA) with DNA and RNA studied with the BIAcore technique. *Biochemistry* **36,** 5072–5077.
8. Nielsen, P. E. (2002) PNA Technology, in *Peptide Nucleic Acids: Methods and Protocols* (Nielsen, P. E., eds.). Humana Press, Totowa, NJ, pp. 3–26.
9. Demidov, V. V., Yavnilovich, M. V., Belotserkovskii, B. P., Frank-Kamenetskii, M. D., and Nielsen, P. E. (1995) Kinetics and mechanism of polyamide ('peptide') nucleic acid binding to duplex DNA. *Proc. Natl. Acad. Sci. USA* **92,** 2637–2641.
10. Egholm, M., Buchardt, O., Christensen, L., et al. (1993) PNA hybridizes to complementary oligonucleotides obeying the Watson-Crick hydrogen-bonding rules. *Nature* **365,** 566–568.
11. Williams, B., Stender, H., and Coull, J. M. (2002) PNA Fluorescent *In Situ* Hybridization for Rapid Microbiology and Cytogenetic Analysis, in *Peptide Nucleic Acids: Methods and Protocols* (Nielsen, P. E., eds.), Humana Press, Totowa, NJ, pp. 181–193.
12. Nuovo, G. J. (2000) In Situ Localization of PCR-Amplified DNA and cDNA, in In Situ *Hybridization Protocols* (Darby, I. A., eds), Humana Press, Totowa, NJ, pp. 217–238.
13. King, G., Payne, S., Walker, F., and Murray, G. I. (1997) A highly sensitive detection method for immunohistochemistry using biotinylated tyramine. *J. Pathol.* **183,** 237–241.
14. Tani, Y. (1999) PCR in situ amplification and catalyzed signal amplification: approaches of higher sensitive, non-radioactive in situ hybridization. *Acta. Histochem. Cytochem.* **32,** 261–270.
15. Murakami, T., Hagiwara, T., Yamamoto, K., et al. (2001) A novel method for detecting HIV-1 by non-radioactive in situ hybridization: application of a peptide nucleic acid probe and catalysed signal amplification. *J. Pathol.* **194,** 130–135.
16. Nakajima, N., Ionescu, P., Sato, Y., et al. (2003) In situ hybridization AT-tailing with catalyzed signal amplification for sensitive and specific in situ detection of human immunodeficiency virus-1 mRNA in formalin-fixed and paraffin-embedded tissues. *Am. J. Pathol.* **162,** 381–389.

High frequency and proliferation of $CD4^+FOXP3^+$ Treg in HIV-1-infected patients with low CD4 counts

Xiuqiong Bi[1], Yasuhiro Suzuki[2], Hiroyuki Gatanaga[1] and Shinichi Oka[1]

[1] AIDS Clinical Center, International Medical Center of Japan, Tokyo, Japan
[2] Department of Infectious and Respiratory Diseases, Tohoku University, Miyagi, Japan

The frequency of Treg is reported to be higher in patients with chronic HIV type 1 (HIV-1) infection and $CD45RA^+$ Treg exist in normal adults. In this study, we found a lower absolute number (15 cells/μL) but a higher proportion (16.2%) of $FOXP3^+$ cells (Treg) in the $CD4^+$ population in treatment-naïve HIV-1 patients with low CD4 (<200 cells/μL) counts than in those with high CD4 counts (34 cells/μL and 9.3%) or healthy adults (48 cells/μL and 7.5%). In HIV-1 patients, $CD45RA^+CCR7^+$, $CD45RA^-CCR7^+$, and $CD45RA^-CCR7^-$ subsets were identified in the Treg population, and the proportion of $CD45RA^-CCR7^-$ Treg was higher (57.9%) in patients with low CD4 than high CD4 counts (38.3%). Treg were in a high proliferation state especially in patients with low CD4 counts. HIV viral load correlated positively with the Treg proliferation rate and the proportion of $CD45RA^-CCR7^-$ Treg. Furthermore, the proliferation of Treg correlated positively with the $CD45RA^-CCR7^-$ Treg proportion but negatively with Treg numbers. Successful antiretroviral therapy resulted in a limited increase in Treg numbers, but their frequency was reduced in 1–2 months due to a rapid rebound of $FOXP3^-$ $CD4^+$cells. Our results suggest that HIV-activating Treg may be a reason for the high frequencies of Treg and $CD45RA^-CCR7^-$ Treg in the peripheral blood of late-stage HIV-1-infected patients.

Key words: Cell proliferation · HIV · Immune regulation · Treg

Supporting Information available online

Introduction

HIV type 1 (HIV-1) infection is characterized by a progressive loss and dysfunction of $CD4^+$ T cells [1, 2]. With regard to reduced T-cell functions, accumulating evidence suggests that the balance between the immune suppression function of natural Treg cells and the effector functions of other types of lymphoid cells influences the magnitude of immune reactions in various types of infections, *e.g.* those caused by *Leishmania major*, *Shistosoma mansonia*, and hepatitis C virus [3–7]. FOXP3 is not only a specific marker but also a critical lineage specification factor for Treg [8–11]. Treg are considered mainly as $CD45RA^-$ cells. However, recent studies have shown that $CD45RA^+$ cells also exist among immune-suppressing $CD25^+CTLA4^+CD4^+$ T cells in adults [12, 13].

The local interaction between Treg and other T cells plays an important role in immune suppression and the local density of Treg determines the course of immune responses to infections [4, 7, 14]. Thus, Treg can be both detrimental and beneficial to the host in response to pathogens [5, 7]. For example, in HIV-infected patients, $CD4^+CD25^+$ Treg have been reported to be proportionally increased, decreased, or highly increased in tonsils, their numbers to correlate with HIV viral load, and to exhibit suppression activity [15–23]. Furthermore, antiretroviral

Dr. Shinichi Oka
e-mail: oka@imcj.hosp.go.jp

therapy (ART) has been reported to have either a negative or no influence on Treg or expression of FOXP3 [18, 23]. In HIV-1-infected individuals, immunodeficiency is often considered when the CD4 cell count falls below 200 cells/μL [1]. However, to our knowledge, there is controversy or little information about the absolute number, frequency, and status of homing markers of Treg in HIV-1-infected patients especially in those with low CD4 counts and late-stage AIDS-related diseases or not on ART [24, 25]. Little is known about the dynamic changes of Treg after ART has been introduced.

It is considered that the CCR7 molecule on T cells is an essential trafficking factor for T cells homing to lymphoid tissues as well as an important marker for defining differentiation stage of T cells with CD45RA molecule [26–28].

The present study was designed to investigate Treg in late-stage HIV-1-infected patients with CD4 count <200 cells/μL and the early impact of ART on Treg. We used the chemokine receptor CCR7 and CD45RA molecules to characterize distinct population of migratory Treg.

Results

High-frequency but low absolute numbers of Treg in HIV-1 patients with low CD4 counts

In this study, we enrolled 95 HIV-1-infected patients and 21 HIV-1-negative Japanese adults as our subjects. Because most AIDS-related diseases occur in HIV-1 patients when their CD4 count decreases to below 200 cells/μL, we classified the patients into two groups, a low CD4 group with a $CD4^+$ T cell count less than 200 cells/μL and a high CD4 group with a $CD4^+$ T cell count not less than 200 cells/μL, for some comparison analysis. Table 1 lists the demographic and clinical characteristics of HIV-1-infected patients and healthy HIV-1-negative controls.

Although FOXP3 expression is considered as the best and most specific marker of Treg, some studies have reported that CD127 and CD25 could distinguish Treg [29, 30]. Accordingly, we first compared the staining of FOXP3 with CD25 and CD127 using PBMC from HIV-1-positive individuals. As shown in Supporting Information Fig. 1A and B, $CD25^+CD127^-$ were a proportion of the CD4 cells. However, gating these cells as Treg seems difficult because of the smear staining of both CD25 and CD127. However, gating FOXP3 in CD4 cells was much easier because of the clear staining of FOXP3. Furthermore, we tested the correlation of the Treg by the two classification markers. Supporting Information Fig. 1C shows a good correlation between the proportion of $FOXP3^+$ and $CD25^+$ $CD127^-$ in CD4 cells in 18 HIV-1 patients. Therefore, in the present study, we considered the $FOXP3^+CD4^+$ cells as Treg, and called $FOXP3^-CD4^+$ cells as conventional $CD4^+$ T cells (Tcon).

In the next step, we investigated the frequency and absolute number of Treg in HIV-1-infected individuals without an ART history and compared them with those of healthy Japanese adults. Figure 1A and B shows FOPX3 expression in $CD4^+$ cells. As shown in Table 2, the proportion of Treg in CD4 cells was $16.2 \pm 2.6\%$ in HIV-1 patients with a low CD4 count and

Table 1. Demographic and clinical characteristics of subjects

	Group[a]		
	A (low CD4)	B (high CD4)	H (healthy)
Characteristics			
Numbers	27	68	21
Age (years, range)	39 (21–65)	38 (21–67)	38 (21–60)
Gender (male:female)	27:0	16:1	3:4
CD4 count (cells/μL, SD)	102 (58)	383 (164)	650 (178)
LogVL (SD)	5 (0.6)	4.2 (0.7)	N/A
AIDS-related diseases[b] (*n*, %)	23 (85)	11 (16)	N/A
Months of HIV^+ (range)[c]	12.3 (0–97)	21 (0–124)	N/A
Numbers for tests			
Frequency and subsets of Treg[d]	20	39	21
Ki67 staining *versus* FOXP3[e]	11	24	5
CCR7FOXP3 *versus* CD25[f]	3	16	
CD127CD25 *versus* FOXP3[g]	6	12	

[a] Low CD4: <200 cells/μL; high CD4: ≥ 200 cells/μL.
[b] AIDS-related diseases included: candida, herpes simplex virus infection, tuberculosis, pneumocystis jirovici pneumonia, lymphoma (kaposis sarcoma), *etc.*
[c] Months between the date of the first time of consulting the hospital and the date of blood collected.
[d] Table 2 and Fig. 1.
[e] Figure 2 and Supporting Information Fig. 2.
[f] Figure 1C.
[g] Supporting Information Fig. 1.

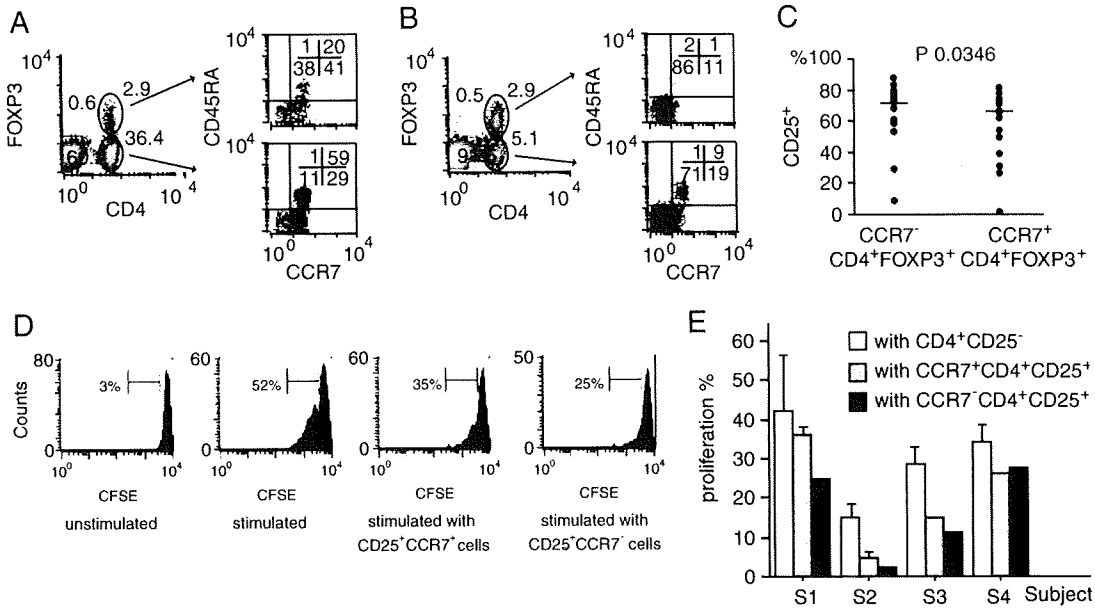

Figure 1. Subsets of Treg in healthy adults and HIV-1-infected patients. (A) Staining of a healthy adult. (B) Staining of an HIV-1-infected patient with low CD4 count. FOXP3 was mainly found in $CD4^+$ T cells both in healthy adults and HIV-1 patients. Treg ($FOXP3^+CD4^+$) cells could be subdivided into $CD45RA^+CCR7^+$, $CD45RA^-CCR7^+$, and $CD45RA^-CCR7^-$ subsets, similar to Tcon ($FOXP3^-CD4^+$, conventional CD4 cells). (C) In HIV-1 patients, the proportion of $CD25^+$ among $CCR7^-$ Treg was higher than that among $CCR7^+$ Treg ($p<0.05$, $n = 19$). (D) A representative proliferation of $CD4^+CD25^-$ responder cells cultured with $CCR7^-CD25^+CD4^+$, $CCR7^+CD25^+CD4^+$ cells, or unlabeled $CD25^-CD4^+$ cells stimulated by anti-CD3 mAb with autologous APC (the data are derived from healthy control). (E) $CCR7^+$ and $CCR7^-$ Treg suppression of responder cells in four subjects. S1–S3: healthy subjects, S4: HIV-1-positive patient (the error bars show duplicate or triplicate tests). Horizontal bars represent median values and p value represents comparison result from Wilcoxon-signed rank test.

$9.3 \pm 0.5\%$ in patients with a high CD4 count. The absolute counts of Treg in low CD4 and high CD4 groups were 15 ± 3 and 34 ± 2 cells/μL, respectively. In healthy adults, the mean CD4 count was 650 cells/μL, and the frequency of Treg among $CD4^+$ cells was $7.5 \pm 0.5\%$ with a mean absolute number of 48 ± 4 cells/μL. Therefore, HIV-1 patients with low CD4 counts had a lower absolute count but a significantly higher frequency of Treg than HIV patients with high CD4 and healthy controls.

High proportion of $CD45RA^-CCR7^-$ Treg in HIV-1 patients with low CD4

Considering the distinct homing potentials and effector functions, CD4 T cells could be subdivided into three subsets, namely naïve ($CD45RA^+CCR7^+$), central memory ($CD45RA^-CCR7^+$), and effector memory ($CD45RA^-CCR7^-$) cells, based on their surface marker and cytokine secretion [26]. Given that local interaction of Treg and Tcon plays an important role in immune suppression and the local number and/or density of Treg reflects immune suppression, we next investigated whether Treg have the same characteristic phenotype as Tcon. Figure 1A shows that Treg could be divided into three subsets, similar to Tcon, based on CD45RA and CCR7 staining in healthy controls. Interestingly, the proportion of each subset of Treg was different compared with the respective subsets of Tcon (Table 2). In healthy adults, the proportion of $CD45RA^-CCR7^-$ Treg ($39.7 \pm 2\%$) was higher than $CD45RA^-CCR7^-$ Tcon cells ($15.6 \pm 1.2\%$), but the proportion of $CD45RA^+CCR7^+$ Treg ($19.3 \pm 1.6\%$) was lower than $CD45RA^+CCR7^+$ Tcon cells ($45.8 \pm 2.4\%$).

In HIV-1-infected patients, the staining patterns of intracellular FOXP3 and surface CD4, CD45RA, and CCR7 were similar to those in healthy controls (Fig. 1A and B). Figure 1B shows a high proportion of $CD45RA^-CCR7^-$ Treg in a representative patient with a low CD4 count. As shown in Table 2, the proportion of $CD45RA^-CCR7^-$ Treg in the low CD4 group ($57.9 \pm 4.2\%$) was significantly higher than in the high CD4 ($38.3 \pm 1.8\%$) or control groups ($39.7 \pm 2\%$). In contrast, the proportion of $CD45RA^-CCR7^+$ Treg in patients with low CD4 counts was significantly lower than in those with high CD4 counts and the control groups. In all subject groups, the proportions of $CD45RA^-$ cells in Treg were higher than in Tcon. Moreover, we found that in HIV-1-infected patients, the proportion of $CD25^+$ in $CCR7^-$ Treg ($64 \pm 19\%$) was higher than in $CCR7^+$ Treg ($58.8 \pm 21\%$, Fig. 1C).

$CD45RA^+$ Treg have been reported to show suppressive function [12]. Based on the finding of a high proportion of $CCR7^-$ Treg in patients with a low CD4 count (Table 2), and considering that $CCR7^+$ cells tend to home to lymphoid tissues whereas $CCR7^-$ cells tend to move to peripheral tissues, we next investigated whether there is any difference in the suppressive activity between $CCR7^+$ and $CCR7^-$ Treg. The results showed

Table 2. Comparison of Treg and Tcon in healthy persons and HIV-1-infected patients[a)]

	Healthy (H)	HIV-1(+)ART(−)		*p* value		
		CD4 < 200 (A)	CD4 ≥ 200 (B)	A *versus* B	A *versus* H	B *versus* H
Number of subjects	21	20	39			
Lymphocytes (cells/μL)	1718 (381)	1028 (447)	1661 (579)	<0.0001	<0.0001	NS
CD4 (cells/μL)	650 (178)	108 (58)	395 (195)	<0.0001	<0.0001	<0.0001
CD4 (%)	38.4 (8.6)	11.4 (7.6)	20.5 (8.5)	0.0001	<0.0001	<0.0001
Treg (cells/μL)	48 (16)	15 (11)	34 (14)	<0.0001	<0.0001	0.0008
Treg (%)	7.5 (2.4)	16.2 (11.8)	9.3 (3.4)	0.0137	0.0004	0.0464
Treg (%)						
$CCR7^+$	57	40.1	59.6	0.0001	0.0029	NS
$CD45RA^+CCR7^+$	19.3	13.4	21.1	0.0109	0.0504	NS
$CD45RA^-CCR7^-$	39.7	57.9	38.3	0.0001	0.0006	NS
$CD45RA^-CCR7^+$	37.7	26.7	38.5	0.0005	0.0057	NS
$CD45RA^-$	77.4	84.6	76.8	0.0131	0.0419	NS
Tcon (%)						
$CCR7^+$	81.3	55.8	74.8	0.0178	0.0035	NS
$CD45RA^+CCR7^+$	45.8	31.9	41.1	NS	0.0217	NS
$CD45RA^-CCR7^-$	15.6	36.8	22.1	0.0283	0.0035	0.04
$CD45RA^-CCR7^+$	35.5	23.9	33.7	0.0048	0.0045	NS
CD45RA	51.1	60.7	55.8	NS	NS	NS
p Value (Treg *versus* Tcon)						
$CCR7^+$	<0.0001	0.0187	<0.0001			
$CD45RA^+CCR7^+$	<0.0001	0.0001	<0.0001			
$CD45RA^-CCR7$	<0.0001	0.0004	<0.0001			
$CD45RA\ CCR7^+$	NS	NS	0.005			
$CD45RA^-$	<0.0001	<0.0001	<0.0001			

[a)] Data are means (SD). NS: not significant. CD4 < 200, CD4 ≥ 200: 200 cells/μL. Mann–Whitney *U*-test was used for comparison between groups (A *versus* B, A *versus* H, B *versus* H). Wilcoxon-signed rank test was used for comparison in group (Treg *versus* Tcon).

that both $CCR7^+$ and $CCR7^-$ $CD25^+CD4^+$ cells suppressed the proliferation of responder cells (Fig. 1D). The suppressive activity was observed in three healthy controls and one HIV-1 patient (Fig. 1E), although no difference was found in the suppression function between the $CCR7^+$ and $CCR7^-$ Treg.

The above results demonstrated the existence of $CD45RA^+$ $CCR7^+$, $CD45RA^-CCR7^+$, and $CD45RA^-CCR7^-$ Treg subsets, similar to Tcon. The proportion of $CCR7^+$ Treg was lower than $CCR7^+$ Tcon cells in both healthy controls and HIV-1 patients. However, the proportion of $CD45RA^-CCR7^-$ Treg was higher than $CD45RA^-CCR7^-$ Tcon, particularly in patients with low CD4 count.

High proliferation of Treg correlates with HIV-1 viral load

Immune cells are activated in HIV-infected patients and such activation is linked to CD4 cell depletion [31]. To determine the mechanism of the high frequency of Treg and $CD45RA^-CCR7^-$ Treg in advanced HIV patients, we stained CD4 cells for the proliferation markers Ki67 in 24 patients (including 11 patients with low CD4 counts and 13 patients with high CD4 counts) and five healthy controls. Figure 2A shows that there was no difference between gating the Ki67 in Treg and Tcon in a healthy control and an HIV-1-infected person. As shown in Fig. 2, the proportions of Ki67-stained cells among Treg in low CD4, high CD4, and control groups (41.7, 24.5, and 22.3%, respectively) were higher than those in Tcon cells (18.1, 11.8, and 7.4%, respectively) (Fig. 2B). The expression of Ki67 in both Treg and Tcon cells was higher in patients with low CD4 counts than in those with high CD4 counts and healthy controls. Furthermore, in the 24 HIV-1-infected patients assessed for Ki67, HIV-1 viral load showed a positive correlation with the frequency of Ki67 in Treg and the proportion of $CD45RA^-CCR7^-$ in Treg. However, the CD4 count showed a negative correlation with the frequency of Ki67 in Treg (Fig. 2C). Moreover, the frequency of Ki67 in Treg correlated negatively with the Treg count and the proportion of $CD45RA^+CCR7^+$ in Treg, but positively with the proportion of $CD45RA^-CCR7^-$ in Treg (Fig. 2D). The same correlation was also observed in Tcon cells (Supporting Information Fig. 2).

ART reduces the frequency of Treg

In HIV-1-infected patients, ART can effectively reduce the HIV viral load and improve CD4 counts. In highly active ART-treated patients, a depleted or normalized Treg was observed in